


ORIGINAL ARTICLE

Endoscopy and Procedures

Diagnosis of Hirschsprung disease by analyzing acetylcholinesterase staining using artificial intelligence

Yannick Braun¹  | Florian Friedmacher¹ | Till-Martin Theilen¹ |
Henning C. Fiegel¹ | Katharina Weber^{2,3,4,5} | Patrick N. Harter^{2,6} | Udo Rolle¹

¹Department of Pediatric Surgery and Pediatric Urology, University Hospital Frankfurt, Goethe-University, Frankfurt am Main, Germany

²Neurological Institute, Edinger Institute, Neuropathology, Goethe University, Frankfurt am Main, Germany

³German Cancer Consortium (DKTK), Partner Site Frankfurt, German Cancer Research Center (DKFZ), Heidelberg, Germany

⁴Frankfurt Cancer Institute (FCI), Frankfurt am Main, Germany

⁵Center for Tumor Diseases, University Hospital Frankfurt, Goethe University, Frankfurt am Main, Germany

⁶Centre for Neuropathology and Prion-Research, Ludwig-Maximilians-Universität München, München, Germany

Correspondence

Yannick Braun, Universitätsklinikum Frankfurt Theodor-Stern-Kai 7, 60590 Frankfurt am Main, Germany.
Email: y.braun@med.uni-frankfurt.de

Funding information

None

Abstract

Objectives: Classical Hirschsprung disease (HD) is defined by the absence of ganglion cells in the rectosigmoid colon. The diagnosis is made from rectal biopsy, which reveals the aganglionosis and the presence of cholinergic hyperinnervation. However, depending on the method of rectal biopsy, the quality of the specimens and the related diagnostic accuracy varies substantially. To facilitate and objectify the diagnosis of HD, we investigated whether software-based identification of cholinergic hyperinnervation in digitalized histopathology slides is suitable for distinguishing healthy individuals from affected individuals.

Methods: $N = 190$ samples of 112 patients who underwent open surgical rectal biopsy at our pediatric surgery center between 2009 and 2019 were included in this study. Acetylcholinesterase (AChE) stained slides of these samples were collected and digitalized via slide scanning and analyzed using two digital imaging software programs (HALO, QuPath). The AChE-positive staining area in the mucosal layers of the intestinal wall was determined. In the next step machine learning was employed to identify patterns of cholinergic hyperinnervation.

Results: The area of AChE-positive staining was greater in HD patients compared to healthy individuals ($p < 0.0001$). Artificial intelligence-based assessment of parasympathetic hyperinnervation identified Hirschsprung disease with a high precision (area under the curve [AUC] 0.96). The accuracy of the prediction model increased when nonrectal samples were excluded (AUC 0.993).

Conclusions: Software-assisted machine-learning analysis of AChE staining is suitable to improve the diagnostic accuracy of Hirschsprung disease.

KEYWORDS

aganglionosis, digital pathology, machine learning, rectal biopsy

1 | INTRODUCTION

Hirschsprung disease (HD) is an intestinal motility disorder caused by the absence of ganglionic cells usually in the most distal part of the colon.¹ The aganglionic segment can be of variant length, up to a total aganglionosis of the colon.² Clinically, HD manifests as severe constipation, which can cause intestinal obstruction and bacterial translocation with subsequent inflammation known as Hirschsprung-associated enterocolitis (HAEC).^{1,3} HD is a

rare congenital disorder that occurs in app. 1.5 in 10,000 live births, with a predominance in males.^{4,5} Upon clinical suspicion of HD, the collection of a rectal tissue specimen is needed to confirm the diagnosis.⁶ Histopathological assessment is performed on respective biopsy specimen to detect the histological features of HD: absence of myenteric and submucosal ganglionic cells, submucosal hypertrophic nerve fibers and parasympathetic mucosal hyperinnervation.⁷ The histopathological workup routinely includes hematoxylin-eosin (HE) staining, as well as a

This is an open access article under the terms of the [Creative Commons Attribution-NonCommercial-NoDerivs](https://creativecommons.org/licenses/by-nc-nd/4.0/) License, which permits use and distribution in any medium, provided the original work is properly cited, the use is non-commercial and no modifications or adaptations are made.

© 2024 The Author(s). *Journal of Pediatric Gastroenterology and Nutrition* published by Wiley Periodicals LLC on behalf of European Society for Pediatric Gastroenterology, Hepatology, and Nutrition and North American Society for Pediatric Gastroenterology, Hepatology, and Nutrition.

spectrum of additional detection methods such as acetylcholinesterase (AChE) histochemistry and immunohistochemistry for calretinin.^{8–11} The quality of the supplied biopsy material has a high influence on the accuracy of the diagnosis. Different means to obtain a sufficient biopsy specimen are employed to varying extents, and two main procedures are used: rectal suction biopsy (RSB) and full-thickness biopsy. RSB is the preferred method of use in many institutions because it can be carried out without the need for general anesthesia and therefore can be performed in the ward or on an outpatient basis.¹² However, RSB is not performed by some pediatric surgeons because of the risk of insufficient yield of submucosal tissue, which may result in an inadequate sample size and thus failure to make a histopathological diagnosis.^{13,14} Subsequently, repeated RSB or full-thickness biopsy is required, which can lead to additional complications, prolonged hospital stay and possibly increased costs. Therefore, some institutions opt for full-thickness biopsy as a primary technique as the risk of insufficient biopsy specimens is reduced.¹⁵ The disadvantages of full-thickness biopsy include the requirement for general anesthesia and the technical difficulty in small neonates. Regardless of the means of biopsy, obtaining a secure diagnosis from a tissue sample with a scarce submucosal specimen is difficult.⁶ Parasympathetic mucosal hyperinnervation is a histopathological feature of HD that is not dependent on the presence of submucosal tissue. However, the assessment of hyperinnervation is subjective and requires a pathologist experienced in the diagnosis of HD. The use of digital pathology and artificial intelligence (AI)-based image analyses has been extensively studied under different conditions, and these methods have shown promise in identifying histopathological findings.^{16,17} For example, in HD, the detection of ganglionic cells and hypertrophic nerve fibers could also be aided using these methods.¹⁸ The aim of this study was to investigate whether the sole investigation of parasympathetic mucosal hyperinnervation supported by digital pathology and AI could aid in the diagnosis of HD.

2 | MATERIALS AND METHODS

2.1 | Patient data

All patients who underwent rectal and colon biopsy at our institution between 2009 and 2019 were included in the study. The inclusion criteria were (1) age under 18 years, (2) available AChE slides, and (3) diagnosis established via biopsy. A total of 131 patients with 283 samples and resulting AChE slides were initially included in the study. The quality and feasibility of the digital workup were assessed. Slides of subpar quality (large air bubbles, foreign material, no mucosal tissue) that were not suitable for digital pathology were excluded (93 slides). The remaining 190 slides

What is Known?

- In the diagnosis of Hirschsprung disease rectal biopsy accuracy and re-biopsy frequency is influenced by the methods of biopsy and tissue availability.
- Analysis of Acetylcholinesterase staining is routinely employed but remains subjective in its evaluation and not disease-specific.
- Artificial intelligence can be useful in pathologic diagnosis but relies on sufficient tissue.

What is New?

- Solely quantitative analysis of acetylcholinesterase staining by digital pathology validates subjective assessment of staining between afflicted and nonafflicted specimens.
- Identification of cholinergic hyperinnervation by machine learning on acetylcholinesterase staining identifies Hirschsprung disease with high accuracy and permits diagnosis in low tissue yield samples.

(=samples) of 112 patients were included in the final analyses. Epidemiologic data (age at biopsy, sex), as well as biopsy data (number of samples, location [colon vs. rectum], and distance to the pectinate line) were recorded.

2.2 | Ethics

The local ethics committee (Ethik-Kommission des Fachbereichs Medizin der Goethe-Universität Frankfurt am Main; Geschäfts-Nr.: 19-444) approved this study. All procedures were in accordance with the 1964 Helsinki Declaration and its later amendments.

2.3 | Tissue and staining

After biopsy collection, the specimen was placed on gauze drenched with 0.9% saline and immediately transported to the pathology unit. Upon arrival, the specimens were frozen in liquid nitrogen. Ten-micron sections of these fresh frozen samples were cut using a cryotome, placed on SuperFrost-Plus slides (Thermo Fisher Scientific) and stored in the freezer overnight. For AChE staining, the sections were dried for 10 min at room temperature and then incubated for 90 min at 37°C in staining solution consisting of 36 mL of freezing medium and 4 mL of 0.005 M potassium ferricyanide (composition: 165 mL of potassium hexacyanide and 100 mL of distilled water).

After incubation, the specimen was rinsed with distilled water and swirled in 96% and 100% alcohol. This was followed by a 10-s incubation in hematoxylin solution, a bluing of the sections under tap water and a final rinse under distilled water. The hematoxylin stain was used as a counterstain to visualize non-AChE-positive tissue (cell nuclei), to allow a more accurate visual representation of the tissue and normalize AChE-positive tissue to the cell number (colocalized tissue). Finally, the sample sections were covered with water using an Aquatex.

Three separate solutions were prepared to prepare the freezing medium for AChE staining. The first solution was composed of 500 mg of acetylcholine iodide, 5.14 g of anhydrous 0.06 M sodium acetate and 725 mL of distilled water. The second solution was prepared using 1.43 g of 0.1 M trisodium citrate-2-hydrate and 50 mL of distilled water. One hundred milliliters of distilled water and 750 mg of copper sulfate \times 5J20 0.03 M were used to prepare the third solution.

These three solutions were mixed, after which 25 mL of an iso-ompa solution consisting of 250 mg of tetraisopropyl pyrophosphoramidate and 182 mL of distilled water was added. The pH was subsequently adjusted to 5.5 with the aid of 7 drops of glacial acetic acid. The staining medium was mixed in 36 mL sections, which were frozen for storage.

2.4 | Digital pathology

The slides were digitalized using a Carl Zeiss Slide Scanner (Carl Zeiss) in the brightfield mode, and the resulting whole-slide images (WSIs) were imported into commercially available (HALO) and open-source software (QuPath v0.2.0) for viewing and further assessment¹⁹ (Figure 1A). Manual annotation of the region was carried out by an investigator (Y.B.) blinded to the diagnosis. HALO was used exclusively for stained area detection. In detail, first, the “general settings” were adjusted to match the image data (resolution, image type [brightfield]). A region of interest (ROI) of a representative size (mean area size of 512,803 μm^2) containing only the mucosal layer and the lamina muscularis mucosae was selected (Figure 1B). In this area, a representative pixel of AChE staining, hematoxylin staining, and background was selected to define the staining vectors. Staining vectors were defined by choosing representative pixels of staining intensity to normalize visual representation of the stained slides across different samples for the annotation and calculation of a mean. After the definition of staining vectors on all slides, the staining vector means were generated and defined as the base for the following analyses on all slides to determine the staining intensity and further analyses. The area stained with AChE (Figure 1C), the area stained with hematoxylin (Figure 1D) and the area

positive for both stains (colocalized area = pixels with an overlay of both stains) (Figure 1E) were measured as a percentage of the selected ROI.

2.5 | AI-classifier training and application

QuPath was used for a supervised AI-based detection of parasympathetic hyperinnervation in rectal biopsies. In detail, the “general settings” were again adjusted to match the image data (resolution, image type [brightfield - other]). Automatic staining detection by automated staining vector estimation was used for each slide, and the brightness of the image was adjusted if necessary. A pixel classifier was trained each time using a subset of 70 images (512 \times 512 pixels) of the mucosal region of 20 HD patients and 120 images (512 \times 512 pixels) of the mucosal region of 40 normal bowel patients (training cohort). Analyses were carried out with 10-fold cross-validation, and the training sets were altered accordingly. For each test run and further cross-validation, only one sample per patient was included in the analyses. Random forest was employed as the algorithm, the resolution chosen was full (0.22 μm per pixel), and the parameters chosen are shown in Supporting Information S1: Suppl. Table 1. A representative mucosal layer ROI of an adequate size (mean ROI area 463,701 μm^2) was chosen manually from the remaining slides not used for classifier establishment (test cohort). The trained pixel classifier was applied to this region, and the amount of positive tissue area was measured as a percentage of the selected ROI (Figure 1F).

2.6 | Statistical analyses and data visualization

All the statistical analyses were performed using JMP11/14 (SAS). Differences were considered significant if $p < 0.05$. Parametric data were tested using Student's *t* test. Categorical variables were tested using Fisher's exact test if the expected frequency of at least one variable was below 5, else using χ^2 test. Nonparametric distributed data were tested using the Wilcoxon test to compare aganglionic bowel tissue with normal bowel tissue.

3 | RESULTS

3.1 | Patient characteristics

Of the 112 patients included in the study, 47 (41.9%) had histopathological features of HD. During the follow-up, 45 patients were treated for “classical” HD,

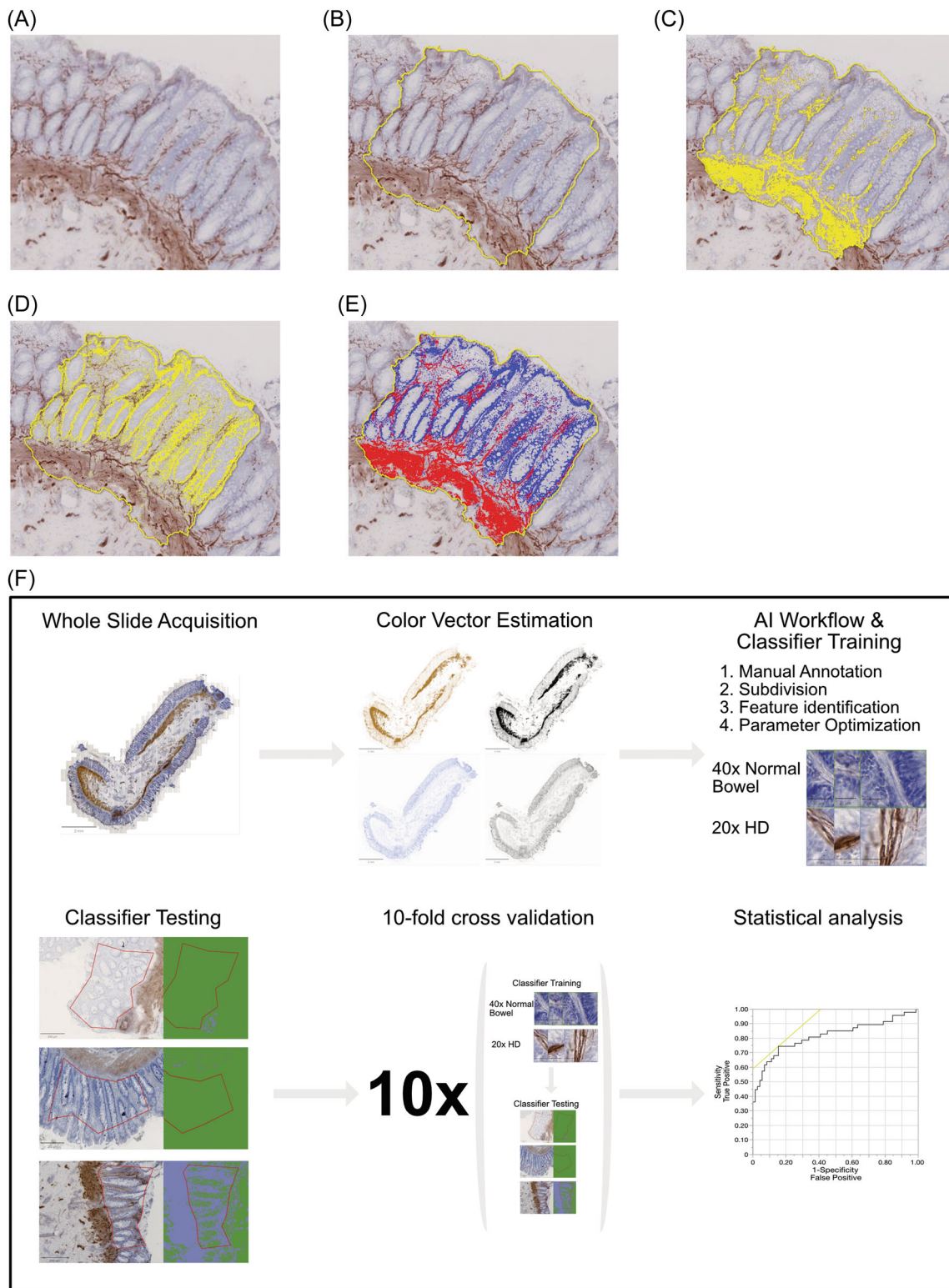


FIGURE 1 (A) Exemplary area of the mucosal layer of a rectal biopsy sample. (B) Selected region of interest outlined by the yellow line. (C) AChE-positive tissue, shown as the yellow area. (D) Hematoxylin-positive region shown as the yellow area. (E) Fusion image with AChE-positive tissue (red area) and hematoxylin-positive tissue (blue area). (F) Artificial intelligence workflow. AChE, acetylcholinesterase.

while two patients had total colonic aganglionosis consistent with Zuelzer-Wilson syndrome. As expected, there was a significant association between male sex and a biopsy consistent with aganglionosis (odds ratio

[OR] 4.32, $p = 0.018$) (Table 1). Patients diagnosed with aganglionosis were, on average, significantly younger than patients with a normal ganglion cell distribution at the time of biopsy (200.5 vs. 1973.8

TABLE 1 Clinical data of analyzed cohort.

All patients, <i>n</i> = 112	Aganglionic bowel <i>n</i> = 47	Normal bowel <i>n</i> = 65	<i>p</i> Value
Male/female sex, <i>n</i> (%)	40 (85.1)/7 (14.9)	37 (56.9)/28 (43.1)	0.018
Age at biopsy in days, mean (Std. Dev.)	200.5 (221.6)	1973.8 (196)	<0.0001
All samples, <i>n</i> = 190	Aganglionic bowel <i>n</i> = 82	Normal bowel <i>n</i> = 108	
Number of samples, mean (Std. Dev.)	2.34 (0.1)	2.37 (0.1)	0.8181
Location of the biopsy: colon/rectum, <i>n</i> (%)	7 (8.5)/75 (91.5)	17 (15.7)/91 (84.3)	0.1862
Distance to the pectinate line in cm, mean (Std. Dev.)	2.4 (0.19)	2.7 (0.18)	0.2403

mean age in days, $p < 0.0001$) (Table 1). In contrast, there was no significant difference between the groups in terms of the average number of samples (2.34 vs. 2.37, $p = 0.8181$), the location of the biopsy (colon/rectum) ($p = 0.1862$) or the mean distance to the pectinate line (2.4 cm vs. 2.7 cm, $p = 0.2403$) (Table 1).

3.2 | The AChE-positive area is increased in HD

First, we analyzed whether the assessment of AChE-positive tissue without regard for morphological features was able to distinguish between HD and normal bowel tissue. The median AChE-positive area was significantly greater in samples with confirmed aganglionosis compared with samples with normal ganglionic cell content and distribution (21.6% vs. 12.55%, $p < 0.0001$) (Figure 2A). Accordingly, the median percentage of colocalized tissue area was greater in HD specimens (1.98% vs. 0.31%, $p < 0.0001$) (Figure 2B). As expected, the hematoxylin-positive area did not significantly differ between the two groups (34.1% vs. 36.65%, $p = 0.8195$) (Figure 2C). We performed simple logistic regression analysis for the prediction of HD by examining the AChE-positive tissue area and colocalized tissue area (Figure 3A,B). The area under the curve (AUC) of the receiver operating characteristic (ROC) curves was 0.816 for AChE-positive tissue and 0.86 for colocalized tissue. Interestingly, if the analyses were limited to only rectal biopsy samples, the AUC of AChE-positive tissue improved to 0.883, while the AUC for colocalized tissue remained relatively the same at 0.867 (Figure 3C,D).

3.3 | High-accuracy AI-based detection of parasympathetic hyperinnervation in identifying HD

In the next step, we aimed to identify parasympathetic hyperinnervation in the mucosal layer by AI-based assessment of AChE staining and staining morphology using the described methodology (Figure 1F). The parasympathetic hyperinnervation scores were significantly greater in HD patients than in healthy individuals across all 10-fold validation cohorts. The mean AUC of the ROC curves after simple logistic regression was 0.959 ± 0.026 , indicating that the classifier identified HD with high accuracy (Figure 3E). This improved again after exclusion of colon biopsies, as the AUC reached 0.993 ± 0.008 (Figure 3F).

4 | DISCUSSION

The accurate diagnosis of Hirschsprung disease relies on several histopathological features assessed by an experienced pathologist.⁶ If sufficient tissue material is available, HE and AChE staining performed on fresh frozen sections alone will allow a rapid and confident diagnosis in most cases.²⁰ However, there are significant pitfalls in biopsy collection that can complicate this process.²¹ Many additional histopathological methods have been developed to aid in the diagnostic process.^{22–24} However, most of these methods involve simplifying the detection of ganglionic cells or hypertrophic nerve fibers. For both, sufficient submucosal tissue is needed. In this study, we showed that if mucosal parasympathetic hyperinnervation, as detected by AChE staining, is analyzed using digital pathology and machine learning, it can distinguish aganglionic from normal bowel tissue with high accuracy.

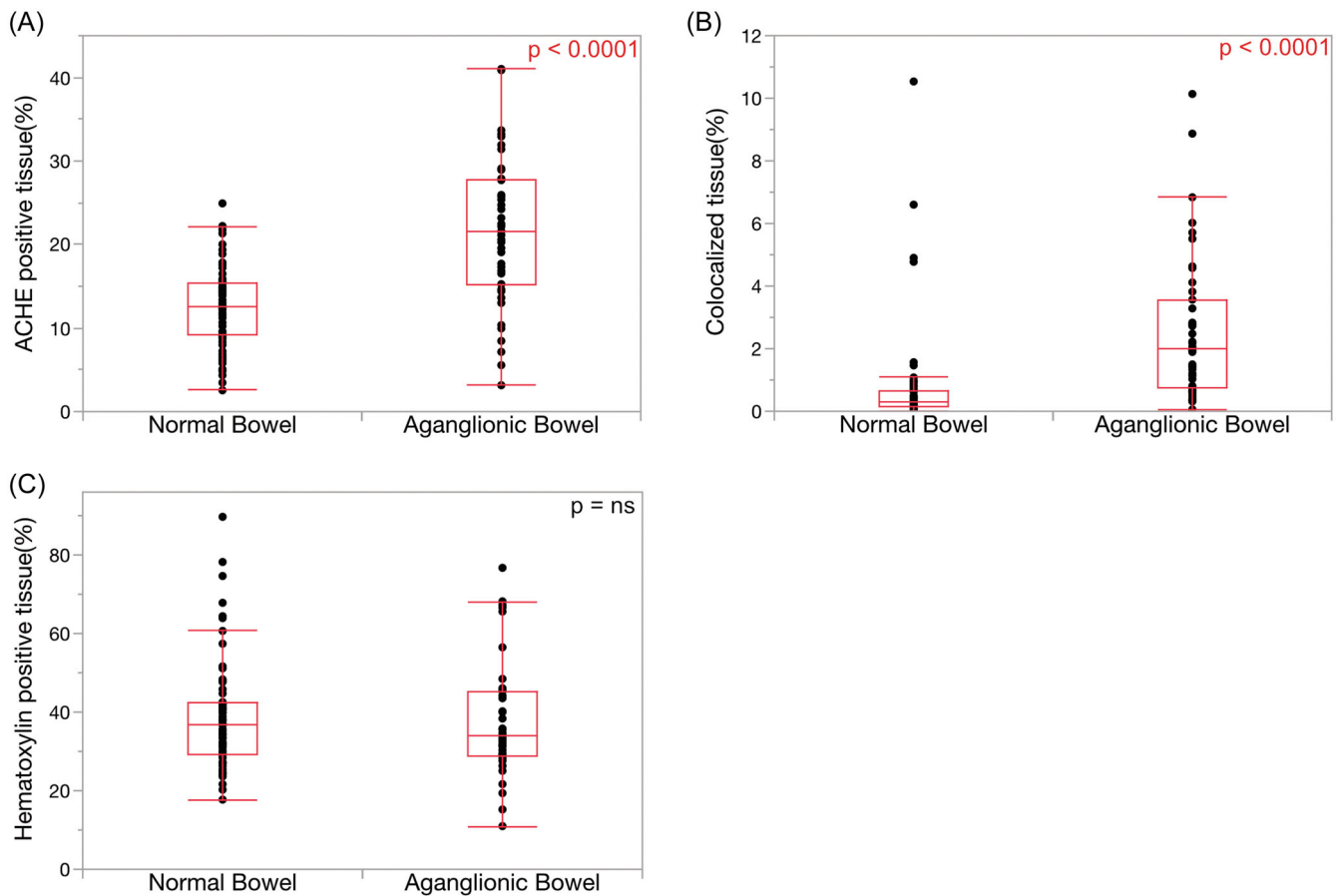


FIGURE 2 (A) AChE-positive tissue area in the normal bowel compared to the aganglionic bowel. (B) Colocalized (double-positive) tissue area in the normal bowel compared to the aganglionic bowel. (C) Hematoxylin-positive tissue area in the normal bowel compared to the aganglionic bowel. AChE, acetylcholinesterase.

Our analyses show that AChE activity was greater in the mucosal tissue and lamina muscularis mucosae of the aganglionic bowel than in the normal bowel. Additionally, colocalized tissue area, which was used as a method to exclude potential non-specific AChE on the luminal area of the mucosal layer was also significantly increased in samples from patients suffering from HD. These findings complement the available literature indicating that parasympathetic hyperinnervation by AChE-positive nerve fibers in the mucosal layer is a histopathological staple of HD.^{9,25,26} Nevertheless, there was, to some extent, detectable enzymatic activity of AChE in normal bowel samples. Kapur et al. and Beltman et al. suggested that subjective evaluation of AChE by pathologists can lead to a misdiagnosis and is inferior to calretinin immunohistochemistry.^{27,28} Accordingly, our results showed that evaluating the AChE-positive area alone can aid in diagnosis, but the AUC of the ROC curves remains less than 90%, highlighting that a considerable number of false-positive results must be accepted to reach a low number of false-negative predictions.

Therefore, we opted to employ a machine learning-based evaluation of parasympathetic hyperinnervation. The use of AI in a variety of image-based analyses has increased in recent years due to its obvious advantages—speed and objectivity of the analyses.^{16,17} Several studies have investigated the use of AI in the diagnostic process of HD. For example, Huang et al. analyzed barium enema images and clinical information with the help of machine learning algorithms (support vector machine and L2-regularized logistic regression) and reported improvements in the accuracy of prebiopsy diagnosis.²⁹ Additionally, AI-based histopathological analyses of HD biopsies have also been performed. Schilling et al. analyzed the expression of a panel of immunohistochemical stains (S100, GLUT1, MAP2, and calretinin) on biopsies as well as resected colon tissue from 27 patients by an ensemble voting classifier, the results of which indicated that the diagnostic accuracy of HD was acceptable in their cohort (sensitivity of 87.5%, specificity of 80%).³⁰ Greenberg et al. developed an AI-based algorithm capable of detecting ganglionic cells in digitalized slides of H.-E.-stained colon specimens with

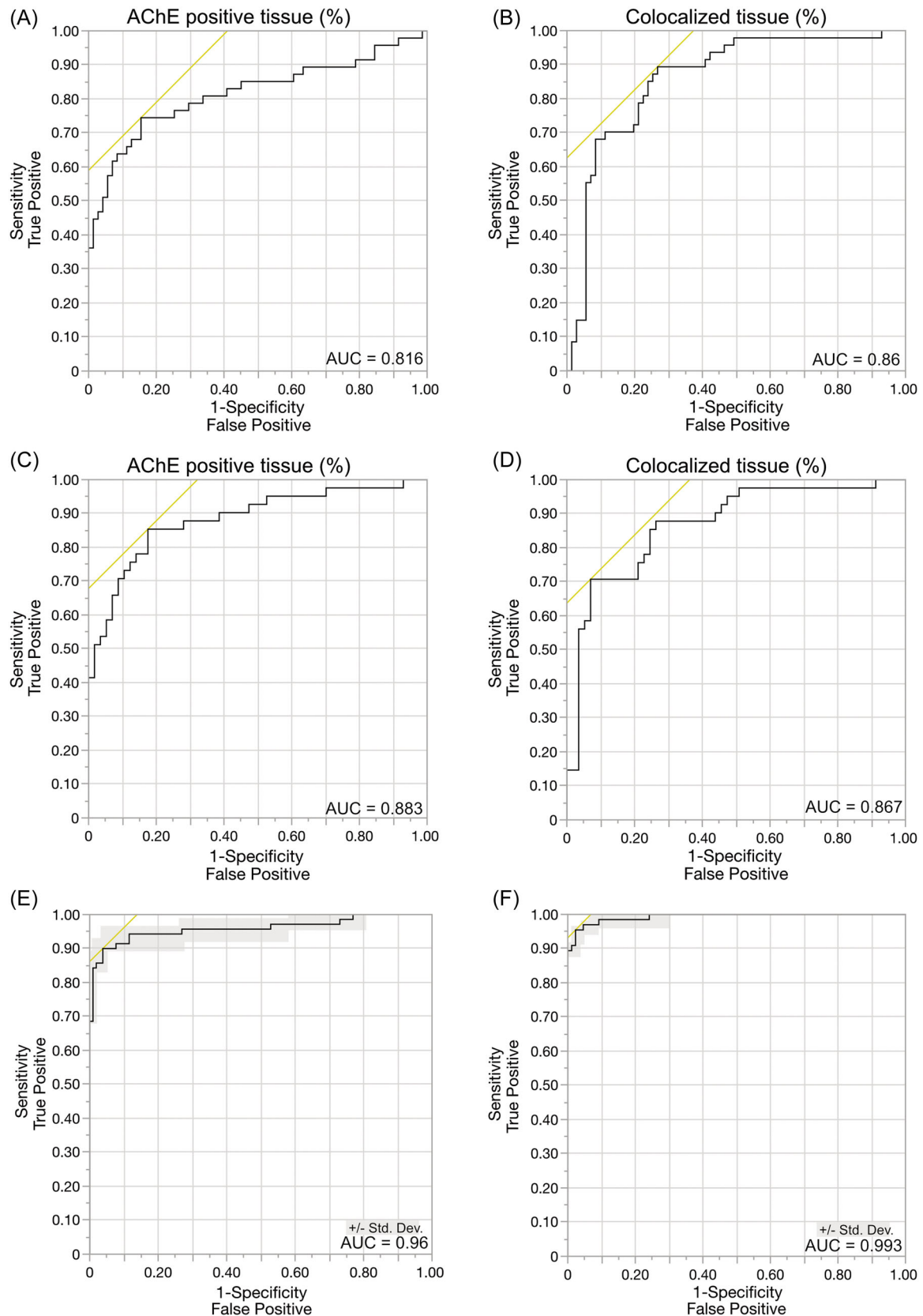


FIGURE 3 ROC curves for simple logistic regression for the prediction of HD based on the (A) AChE-positive tissue area, (B) colocalized (double-positive) tissue area, (C) AChE-positive tissue area in rectal samples only, (D) the colocalized (double-positive) tissue area in rectal samples only, (E) parasympathetic hyperinnervation as determined by artificial intelligence, and (F) parasympathetic hyperinnervation determined by artificial intelligence in rectal samples only. AChE, acetylcholinesterase; HD, Hirschsprung disease; ROC, receiver operating characteristic.

high accuracy, even when detecting a previously misdiagnosed case of HD.¹⁸ In a recently published study, Duci et al. demonstrated the diagnostic accuracy of an AI-based U-net classifier detecting ganglionic cells and hypertrophic nerve fibers on formalin-fixed tissue samples analyzed after resection.³¹ Taken together, these findings illustrate the potential of machine learning in the histopathological assessment of HD biopsies.

In our study, we focused on AChE staining, which is routinely performed at most institutions and therefore widely available. Additionally, only marginal specimens of mucosal tissue need to be provided for the analyses. To build our classifier, we utilized QuPath, an open-source digital pathology software package with built-in AI capabilities through its pixel classifier, in which its usage for pattern detection has been previously described. The underlying data set was annotated according to the diagnosis made at the initial assessment by a pathologist experienced in the diagnosis of HD with all available immunohistochemical and enzyme-histochemistry methods at their disposal. Input data were relatively scarce compared to the recommended sizes of the machine learning data sets; however, comparable studies achieved consistent results with similar data set sizes.³²⁻³⁶ We opted for 10-fold cross-validation to diminish the extent of overestimation of our classifier results.³⁷ Different iterations of the classifier using different input selections of image data were initialized (Supporting Information S1: Suppl. Tables 2 and 3; Suppl. Figure 1), and the parameters were altered until the best result was achieved.

The resulting classifier was able to detect HD with high diagnostic accuracy, comparable to or outdoing the findings of previous studies utilizing a variety of methods with the goal of improving the diagnostic accuracy. Most methods still rely on the availability of a substantial amount of submucosal specimen, while our classifier utilizes the mucosal layer only. Interestingly, the diagnostic accuracy of our classifier improved when only rectal biopsy samples were analyzed.

Our study has limitations that warrant discussion. It is a single-institution investigation and therefore has a uniform surgical and histopathological workflow. This leads to low variance in the input data. Therefore, whether our machine learning algorithm is applicable to AChE slides from another institution with a different staining protocol remains to be determined. AChE staining is a method not uniformly carried out in all institutions, limiting the transferability of the results for other investigators. The study was conducted using incisional biopsy samples, a considerable number of institutions rely on suction biopsies to establish their diagnosis, although the analyzed region is contained to the mucosa and therefore also included in these samples a reproducibility on suction biopsy samples is not guaranteed. Additionally, all AI- and machine learning-based approaches rely on accurate input data. All patients diagnosed with HD in our study were surgically

treated, and the diagnosis was corroborated with the analyzed surgical specimen. However, there was no complete exclusion of false-negative diagnoses during the initial assessment. Finally, our classifier depends on the manual annotation of the mucosal region, which may underlie substantial selection bias. To overcome this burden, if possible, multiple regions were annotated, and the annotation was performed by an investigator not trained in the histopathological evaluation of HD and blinded to the diagnosis; however, an effect on the results was not fully excluded.

5 | CONCLUSION

In conclusion, our study shows that even a basic machine learning approach using the built-in AI capabilities of open-source digital pathology software can make enzyme histochemical detection of AChE an even more useful tool for distinguishing affected patients from those with normal bowel innervation and therefore can be used in the establishment of a secure histopathological diagnosis.

ACKNOWLEDGMENTS

The authors have no funding to report. Open Access funding enabled and organized by Projekt DEAL.

CONFLICT OF INTEREST STATEMENT

The authors declare no conflict of interest.

DATA AVAILABILITY STATEMENT

Raw data files are available upon request to the corresponding author.

ORCID

Yannick Braun  <http://orcid.org/0000-0002-2939-4512>

REFERENCES

1. Montalva L, Cheng LS, Kapur R, et al. Hirschsprung disease. *Nat Rev Dis Primers*. 2023;9(1):54.
2. Meier-Ruge W, Hunziker O, Tobler HJ, Walliser C. The pathophysiology of aganglionosis of the entire colon (Zuelzer-Wilson syndrome). Morphometric investigations of the extent of sacral parasympathetic innervation of the circular muscles of the aganglionic colon. *Beitr Pathol*. 1972;147(3):228-236.
3. Gosain A, Frykman PK, Cowles RA, et al. Guidelines for the diagnosis and management of Hirschsprung-associated enterocolitis. *Pediatr Surg Int*. 2017;33(5):517-521.
4. Badner JA, Sieber WK, Garver KL, Chakravarti A. A genetic study of Hirschsprung disease. *Am J Hum Genet*. 1990;46(3):568-580.
5. Best KE, Addor MC, Arriola L, et al. Hirschsprung's disease prevalence in Europe: a register based study. *Birth Defects Res Pt A Clin Molec Teratol*. 2014;100(9):695-702.
6. Ambartsumyan L, Smith C, Kapur RP. Diagnosis of Hirschsprung disease. *Pediatr Dev Pathol*. 2020;23(1):8-22.
7. Feichter S, Meier-Ruge WA, Bruder E. The histopathology of gastrointestinal motility disorders in children. *Semin Pediatr Surg*. 2009;18(4):206-211.

8. Setiadi JA, Dwihantoro A, Iskandar K, Heriyanto DS, Gunadi S. The utility of the hematoxylin and eosin staining in patients with suspected Hirschsprung disease. *BMC Surg.* 2017;17(1):71.
9. Boston VE, Dale G, Riley KWA. Diagnosis of Hirschsprung's disease by quantitative biochemical assay of acetylcholinesterase in rectal tissue. *Lancet.* 1975;306(7942):951-953.
10. Yoshimaru K, Yanagi Y, Obata S, et al. Acetylcholinesterase staining for the pathological diagnosis of Hirschsprung's disease. *Surg Today.* 2021;51(2):181-186.
11. Barshack I, Fridman E, Goldberg I, Chowers Y, Kopolovic J. The loss of calretinin expression indicates aganglionosis in Hirschsprung's disease. *J Clin Pathol.* 2004;57(7):712-716.
12. Friedmacher F, Puri P. Rectal suction biopsy for the diagnosis of Hirschsprung's disease: a systematic review of diagnostic accuracy and complications. *Pediatr Surg Int.* 2015;31(9):821-830.
13. Vervloet G, De Backer A, Heyman S, et al. Rectal biopsy for Hirschsprung's disease: A multicentre study involving biopsy technique, pathology and complications. *Children.* 2023;10(9):1488.
14. Friedmacher F, Puri P. Current practice patterns of rectal suction biopsy in the diagnostic work-up of Hirschsprung's disease: results from an international survey. *Pediatr Surg Int.* 2016;32(8):717-722.
15. Bjørn N, Rasmussen L, Qvist N, Detlefsen S, Ellebæk MB. Full-thickness rectal biopsy in children suspicious for Hirschsprung's disease is safe and yields a low number of insufficient biopsies. *J Pediatr Surg.* 2018;53(10):1942-1944.
16. Niazi MKK, Parwani AV, Gurcan MN. Digital pathology and artificial intelligence. *Lancet Oncol.* 2019;20(5):e253-e261.
17. Shmatko A, Ghaffari Laleh N, Gerstung M, Kather JN. Artificial intelligence in histopathology: enhancing cancer research and clinical oncology. *Nature Cancer.* 2022;3(9):1026-1038.
18. Greenberg A, Aizic A, Zubkov A, Borsekofsky S, Hagege RR, Hershkovitz D. Automatic ganglion cell detection for improving the efficiency and accuracy of Hirschsprung disease diagnosis. *Sci Rep.* 2021;11(1):3306.
19. Bankhead P, Loughrey MB, Fernández JA, et al. QuPath: open source software for digital pathology image analysis. *Sci Rep.* 2017;7(1):16878.
20. Kyrklund K, Sloots CEJ, de Blaauw I, et al. ERNICA guidelines for the management of rectosigmoid Hirschsprung's disease. *Orphanet J Rare Dis.* 2020;15(1):164.
21. Hwang S, Kapur RP. Advances and pitfalls in the diagnosis of Hirschsprung disease. *Surg Pathol Clin.* 2020;13(4):567-579.
22. Holland SK, Ramalingam P, Podolsky RH, Reid-Nicholson MD, Lee JR. Calretinin immunostaining as an adjunct in the diagnosis of Hirschsprung disease. *Ann Diagn Pathol.* 2011;15(5):323-328.
23. Kawana T, Nada O, Ikeda K. An immunohistochemical study of glial fibrillary acidic (GFA) protein and S-100 protein in the colon affected by Hirschsprung's disease. *Acta Neuropathol.* 1988;76(2):159-165.
24. Beschorner R, Mittelbronn M, Bekure K, Meyermann R. Problems in fast intraoperative diagnosis in Hirschsprung's disease. *Folia Neuropathol.* 2004;42(4):191-195.
25. Moore SW, Johnson G. Acetylcholinesterase in Hirschsprung's disease. *Pediatr Surg Int.* 2005;21(4):255-263.
26. Elema JD, de Vries JA, Vos LJM. Intensity and proximal extension of acetylcholinesterase activity in the mucosa of the rectosigmoid in Hirschsprung's disease. *J Pediatr Surg.* 1973;8(3):361-368.
27. Kapur RP, Reed RC, Finn LS, Patterson K, Johanson J, Rutledge JC. Calretinin immunohistochemistry versus acetylcholinesterase histochemistry in the evaluation of suction rectal biopsies for Hirschsprung disease. *Pediatr Dev Pathol.* 2009;12(1):6-15.
28. Beltman L, Windster JD, Roelofs JJTH, van der Voorn JP, Derikx JPM, Bakx R. Diagnostic accuracy of calretinin and acetylcholinesterase staining of rectal suction biopsies in Hirschsprung disease examined by unexperienced pathologists. *Virchows Arch.* 2022;481(2):245-252.
29. Huang S, Qian X, Cheng Y, Guo W, Zhou Z, Dai Y. Machine learning-based quantitative analysis of barium enema and clinical features for early diagnosis of short-segment Hirschsprung disease in neonate. *J Pediatr Surg.* 2021;56(10):1711-1717.
30. Schilling F, Geppert CE, Strehl J, et al. Digital pathology imaging and computer-aided diagnostics as a novel tool for standardization of evaluation of aganglionic megacolon (Hirschsprung disease) histopathology. *Cell Tissue Res.* 2019;375(2):371-381.
31. Duci M, Magoni A, Santoro L, et al. Enhancing diagnosis of Hirschsprung's disease using deep learning from histological sections of post pull-through specimens: preliminary results. *Pediatr Surg Int.* 2023;40(1):12.
32. Mondal R, Sandhu YK, Kamalia VM, et al. Measurement of A β amyloid plaques and tau protein in postmortem human Alzheimer's disease brain by autoradiography using [18F]Flotaza, [125I]IBETA, [124/125I]IPPI and immunohistochemistry analysis using QuPath. *Biomedicines.* 2023;11(4):1033.
33. Porter R, Din S, Bankhead P, Oniscu A, Arends M. QuPath algorithm accurately identifies MLH1-deficient inflammatory bowel disease-associated colorectal cancers in a tissue microarray. *Diagnostics.* 2023;13(11):1890.
34. Zheng Q, Jiang Z, Ni X, et al. Machine learning quantified tumor-stroma ratio is an independent prognosticator in muscle-invasive bladder cancer. *Int J Mol Sci.* 2023;24(3):2746.
35. Zhdanovich Y, Ackermann J, Wild PJ, et al. Evaluation of automatic discrimination between benign and malignant prostate tissue in the era of high precision digital pathology. *BMC Bioinform.* 2023;24(1):1.
36. Martino F, Varricchio S, Russo D, et al. A machine-learning approach for the assessment of the proliferative compartment of solid tumors on hematoxylin-eosin-stained sections. *Cancers.* 2020;12(5):1344.
37. Demircioğlu A. Measuring the bias of incorrect application of feature selection when using cross-validation in radiomics. *Insights Imaging.* 2021;12(1):172.

SUPPORTING INFORMATION

Additional supporting information can be found online in the Supporting Information section at the end of this article.

How to cite this article: Braun Y, Friedmacher F, Theilen T-M, et al. Diagnosis of Hirschsprung disease by analyzing acetylcholinesterase staining using artificial intelligence. *J Pediatr Gastroenterol Nutr.* 2024;1-9.
doi:10.1002/jpn3.12339